Triggering and Visualizing the Aggregation and Fusion of Lipid Membranes in Microfluidic Chambers

Daniel J. Estes,* Santiago R. Lopez,† A. Oveta Fuller,†§ and Michael Mayer*‡
*Department of Biomedical Engineering and †Department of Chemical Engineering, College of Engineering, and ‡Department of Microbiology and Immunology and §Program in Cellular and Molecular Biology, School of Medicine, University of Michigan, Ann Arbor, Michigan 48109

ABSTRACT We present a method that makes it possible to trigger, observe, and quantify membrane aggregation and fusion of giant liposomes in microfluidic chambers. Using electroformation from spin-coated films of lipids on transparent indium tin oxide electrodes, we formed two-dimensional networks of closely packed, surface-attached giant liposomes. We investigated the effects of fusogenic agents by simply flowing these molecules into the chambers and analyzing the resulting shape changes of more than 100 liposomes in parallel. We used this setup to quantify membrane fusion by several well-studied mechanisms, including fusion triggered by Ca^{2+}, polyethylene glycol, and biospecific tethering. Directly observing many liposomes simultaneously proved particularly useful for studying fusion events in the presence of low concentrations of fusogenic agents, when fusion was rare and probabilistic. We applied this microfluidic fusion assay to investigate a novel 30-mer peptide derived from a recently identified human receptor protein, B5, that is important for membrane fusion during the entry of herpes simplex virus into host cells. This peptide triggered fusion of liposomes at an ~6 times higher probability than control peptides and caused irreversible interactions between adjacent membranes; it was, however, less fusogenic than Ca^{2+} at comparable concentrations. Closely packed, surface-attached giant liposomes in microfluidic chambers offer a method to observe membrane aggregation and fusion in parallel without requiring the use of micromanipulators. This technique makes it possible to characterize rapidly novel fusogenic agents under well-defined conditions.

INTRODUCTION

The fusion of biological membranes is crucial for life (1): viral fusion, exocytosis, organelle fusion, and fertilization of an oocyte are examples of biological processes that involve the merging of closed membranes. To study the molecular machinery and processes that govern the wide range of fusion events, cellular assays as well as assays in reconstituted systems can yield important insight and may ultimately lead to approaches to interfere with fusion processes for therapeutic purposes (2). Here, we describe a versatile and practical fusion assay that proceeds in microfluidic chambers and makes it possible to investigate individual components of the fusion machinery under well-defined and variable conditions.

Membrane fusion typically involves three conserved steps: i), close contact between two membranes (3); ii), initial merging of the membranes, often associated with a hemifusion state (4); and iii), opening of an aqueous fusion pore (5). In living cells, membrane fusion is facilitated by proteins. Intracellular fusion of membranes involves the tethering of membranes by Rab proteins and the formation of SNARE (soluble *N*-ethylmaleimide sensitive factor attachment protein receptor) complexes to induce fusion (6,7). Fusion by viruses can be mediated by fusion peptides which are typically 15–30 amino acids long. When activated, these peptides insert into the target membrane and trigger fusion (8,9). The regulation of the interactions between proteins, lipids, and other molecules in these cellular processes is complex. Artificial lipid membranes, in contrast, offer systems for studying individual parameters involved in membrane fusion and for determining minimal models of this process (10–12). Weber et al. showed that complementary SNARE proteins reconstituted into separate liposomes were sufficient to induce fusion (13). Other studies employing artificial vesicles have shown that a range of external factors affect fusion, including mechanical stress (14–16), divalent and trivalent cations (17–19), long-chain polymers (20,21), high-strength electric fields (22), and membrane curvature (23–26).

Several techniques have been developed to investigate membrane fusion in artificial systems. Fusion assays typically assess the mixing of lipids and of the contents of liposomes when fusogenic agents are added. These measurements usually employ small liposomes (typically <200 nm) with high radii of curvature and utilize fluorescence techniques (27–30), light scattering (31), or electron microscopy (32,33) for detection. In these assays, the size of liposomes affects fusion; recently, Nomura et al. reported that the hemagglutinin (HA) fusion peptide promoted fusion of liposomes with diameters <200 nm but did not induce fusion of giant liposomes (34).

Fusion assays using cell-sized, giant liposomes allow microscopic observation of membrane fusion and assessments of mixing of lipids and contents. Such experiments

Submitted October 18, 2005, and accepted for publication April 5, 2006.

Address reprint requests to Michael Mayer, University of Michigan, Depts. of Biomedical Engineering and Chemical Engineering, Gerstacker Building, Rm. 1107, 2200 Bonisteel Blvd., Ann Arbor, MI 48109-2099. Tel.: 734-763-4609; Fax: 734-763-4371; E-mail: mimayer@umich.edu.

0006-3495/06/07/233/11 $2.00

doi: 10.1529/biophysj.105.076398

typically use micropipette techniques to bring two liposomes into close contact (17,35). For this approach, liposomes adhere to a micropipette through suction (36), and micromanipulators position the micropipettes to establish contact between two liposomes (37–39). Other methods have utilized electrophoresis to fuse oppositely charged liposomes (40), dielectrophoresis to bring liposomes together for electrofusion (41), or a mixing chamber (34). Here we present a method that affords fusion assays with the following five characteristics: i), it enables direct visualization of membrane aggregation and fusion of cell-sized liposomes in a microfluidic chamber; ii), it monitors hundreds of membrane-membrane contacts in parallel; iii), it allows controlled triggering of fusion by biologically relevant mechanisms under physiological conditions without the need for manual control; iv), it investigates fusion of lipid membranes of well-defined composition in the absence or presence of fusogenic agents; and v), it provides the opportunity to vary the composition of the aqueous environment in which the fusion process occurs.

In previous work, Chiu et al. trapped two cells or liposomes in a microfluidic system (by optical trapping, dielectrophoresis, or micromanipulation) and used high-strength electric fields ($E > 100$ kV·m^{-1}) to fuse the cells (41–44). We adopted a different approach to obtain giant liposomes in close contact by drawing upon techniques recently developed in our lab: we formed densely packed networks of surface-attached giant liposomes in flow chambers (45,46). These liposome networks allowed the introduction of fusogenic molecules to the liposomes in the flow chambers and provided a means to visualize fusion events directly in an optically transparent setup. Unlike most fusion assays with giant liposomes, this setup made it possible to observe many membrane-membrane interactions in parallel. Moreover, it required no micromanipulators to bring liposomes into close contact. We validated this microfluidic fusion assay by triggering fusion with well-studied fusogenic agents such as calcium ions and polyethylene glycol (PEG). We then reconstituted a minimal model of protein-mediated fusion that was based on biospecific interaction between membranes. Finally, we demonstrate the usefulness of this technology by performing a fusion assay on a recently characterized peptide that is involved in the entry of herpes simplex virus (HSV) into host cells. The results show that triggering membrane fusion in microfluidic chambers under well-defined conditions can yield important insight into the fusogenic properties of novel molecules.

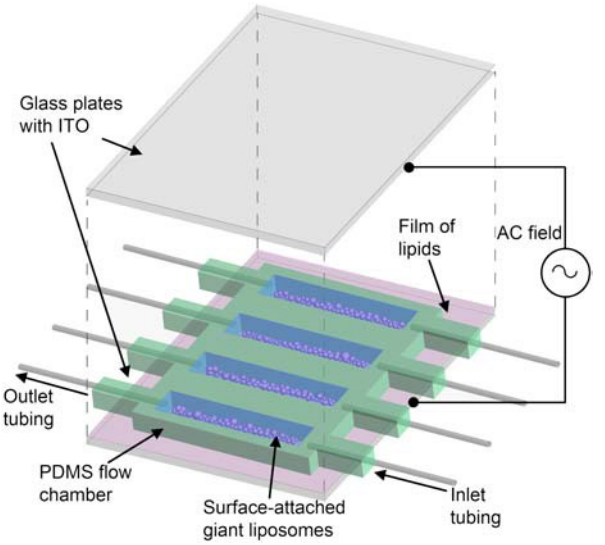

FIGURE 1 Microfluidic setup for forming surface-attached giant liposomes and triggering fusion of these liposomes. A PDMS spacer with embedded silicone tubing leading into and out of four parallel flow chambers was sandwiched between two glass plates each covered with a surface of ITO. Films of lipids were spin coated onto the surfaces of ITO before assembly of the setup. Giant liposomes were formed by electroformation after filling the chambers with solution. An AC electric field was applied to the ITO surfaces over 2 h to form liposomes. This setup was optically transparent and allowed the introduction of new solutions to the chambers at defined flow rates using a microprocessor-controlled syringe pump.

MATERIALS AND METHODS

Preparation of a microfluidic setup for fusion assays

The microfluidic setup used in this work consisted of four parallel flow chambers in which we formed surface-attached giant liposomes (Fig. 1). Detailed methods for fabrication have been described previously (45). Briefly, we embedded four pieces of silicone tubing (inside diameter = 0.60 mm, Dow Corning, Midland, MI) in a slab of 2.1-mm-thick poly(dimethylsiloxane) (PDMS, Sylgard 184 Silicone, Dow Corning) (47) and extracted four rectangular chambers (29.1 mm × 3.24 mm × 2.22 mm, volume = 209 μL) using a surgical blade. This PDMS structure was sandwiched between two large aluminosilicate glass slides (50 mm × 50 mm × 1.1 mm) covered each with a surface of indium tinoxide (ITO, R, = 5-15 ohms. Delta Technologies, Stillwater, MN). The assembly was held together by binder clips (Officemate International, Edison, NJ) (Fig. 1). Before assembly of the setup, we prepared films of lipids by spin coating (46). Solutions of 3.75 mg mL^{-1} lipids (mixtures of L-α-phosphatidylcholine (egg, chicken) (eggPC), 1-palmitoyl-2-oleoyl-*sn*-glycero-3-phosphocholine (POPC), 1-palmitoyl-2-oleoyl-*sn*-glycero-[phospho-rac-(1-glycerol)] (POPG), 1-palmitoyl-2-oleoyl-*sn*-glycero-3-phosphoethanolamine (POPE), and 1,2-dipalmitoyl-*sn*-glycero-3-phosphoethanolamine-*N*-(cap piotinyl) (sodium salt) (*N*-cap biotin-PE) all from Avanti Polar Lipids, Alabaster, AL) in 95% chloroform (Acros Organics, Morris Plains, NJ), 5% acetonitrile (Acros Organics, Geel, Belgium) were spin coated onto ITO at a speed of 600 rpm for 100 s. Films of lipid were dried under vacuum (−740 mTorr) for 2 h to remove traces of solvent. We used the same PDMS flow chambers in all experiments with the wash protocols for the PDMS flow chambers and the plates of ITO as described previously (45,46).

Formation of giant liposomes in microfluidic chambers

We employed electroformation, a technique developed by Angelova and Dimitrov, to form giant liposomes (48,49). Application of alternating current (AC) voltages to electrodes with films of lipids on their surface induces the swelling of giant, unilamellar liposomes from the lipid film (50,51). We hydrated the spin-coated film of lipids in the flow chambers by filling, in succession, each chamber with solution while applying an AC voltage of 1.6 V peak-to-peak (Vpp) at a frequency of 10 Hz using a function generator

(Circuitmate FG2, Beckman Coulter, Fullerton, CA) attached to the ITO electrodes. We allowed electroformation to proceed for 2 h before turning off the electric field.

Flow procedures for triggering fusion

To replace solutions inside the flow chambers, we used a programmable syringe pump (KD Scientific, Holliston, MA) to drive fluid flow at volumetric flow rates below 5.0 mL h^{-1}. For experiments involving Ca^{2+}-induced fusion, we formed giant liposomes from 90% POPC, 10% POPE in solutions of 0.1 mM Tris (hydroxymethyl) aminomethane (Tris, Shelton Scientific, Shelton, CT) buffer pH 7.4. We then introduced 0–100 μM solutions of $CaCl_2$ (EMD Chemicals, Gibbstown, NJ) that contained 0.1 mM Tris buffer at a rate of 2.6 mL h^{-1} to induce fusion.

To examine two-dimensional aggregation of giant liposomes, we formed giant liposomes composed of 100% eggPC in solutions of glycerol that were isoosmolar to the $CaCl_2$ to be introduced to the chamber. Solutions of $CaCl_2$ (ranging from 0.1 μM to 200 mM) were flowed through the chamber of liposomes for 1 h at rates $<$4.0 mL h^{-1}.

For experiments with poly-ethylene glycol (PEG), we employed giant liposomes composed of 90% POPC, 10% POPE. To examine PEG-induced fusion with osmotic mismatches between the inside and outside of liposomes, we formed giant liposomes in 0.1 mM Tris buffer pH 7.4 and introduced 1, 5, and 10 mM PEG-6000 (Calbiochem, San Diego, CA) at 2.0 mL h^{-1} for 1 h. We also performed experiments with osmotically matched solutions of PEG-6000. Using an osmometer (Model 3320, Advanced Instruments, Norwood, MA) to match osmolalities, we formed giant liposomes in solutions of 1, 10, and 38 mM sucrose (EM Industries, Gibbstown, NJ) and then introduced to the chambers 1, 5, and 10 mM PEG-6000, respectively (see Fig. S3 for osmolality concentration curves for PEG-6000 and sucrose). Finally, to compare PEG-6000 to the other fusogenic molecules used in this assay, we introduced 25 μM PEG-6000 in 0.01$\times$ phosphate buffered saline (PBS) to giant liposomes prepared exactly as described below for experiments with the fusion peptide.

For experiments involving ''receptor-mediated'' fusion, we formed giant liposomes composed of 95% POPC, 5% biotinyl-PE in deionized H_2O (diH_2O). We introduced 1.67 μM NeutrAvidin biotin-binding protein (Molecular Probes, Eugene, OR) dissolved in diH_2O at a rate of 2.5 mL h^{-1} to induce fusion.

Fusion assay with peptide from B5 protein

We performed a fusion assay with a synthetic peptide from the C-terminus of the B5 receptor protein that can facilitate entry of HSV into host cells (52). This 30-amino acid peptide (denoted WT-B5 peptide), corresponded to amino acids 344–374 (KQQWQQLYDTLNAWKQNLNKVKNSLLSLSD) of the B5 protein. It was synthesized and purified to 98% by the University of Michigan protein core facility (52). The peptide was acetylated at the N-terminus, amidated at the C-terminus, and dissolved in PBS to a concentration of 2.5 mM. We used two other peptides as control peptides in the fusion assay, the oxidized chain B of insulin from bovine pancreas (Sigma, St. Louis, MO) and human adrenocorticotropic hormone (ACTH) residues 1–24 (AnaSpec, San Jose, CA), dissolved in diH_2O without further modification.

For all fusion assays with WT-B5 peptide, giant liposomes composed of 90% POPC, 10% POPE were formed in 0.1 mM Tris buffer pH 7.4. We prepared solutions of WT-B5 peptide by diluting the stock solutions (2.5 mM WT-B5 peptide in PBS) in diH_2O. In the case of oxidized chain B of insulin and ACTH (1–24), we added PBS to the diluted solutions to match the osmolarity and ionic strength of the solutions of WT-B5 peptide at a given concentration of peptide. Before introducing the solutions of peptides to the liposomes, we flowed solutions of PBS through the chamber of liposomes at 2.5 mL h^{-1} for 1 h to replace the Tris buffer inside and outside of the surface-attached liposomes; we demonstrated previously that new solutions introduced to surface-attached giant liposomes replace the previous solution both outside and inside the liposomes (45). These solutions were isoosmolar to the solution of peptide to be introduced, thus ensuring that osmolarity differences were not a factor in the fusion assay. After filling the chambers with PBS, we introduced the peptide solutions to the chambers at a rate of 2.5 mL h^{-1} for 1 h for all experiments.

Observation and quantification of fusion

We observed giant liposomes and membrane fusion by phase contrast microscopy using an inverted microscope (Eclipse TE 2000-U, Nikon, Melville, NY) with 10$\times$ and 20$\times$ objectives with extra long working distance in phase-contrast mode. We captured images and movies of liposomes using a charge-coupled device camera (Photometrics CoolSnap HQ, Roper Scientific, Trenton, NJ). Image analysis software (Metamorph from Universal Imaging Corporation, Downington, PA) allowed for determination of the size of liposomes. Fusion events were observable and could be quantified by visually examining movies frame-by-frame for the occurrence of merging of liposomes (see Supplementary Material for movies).

In the fusion assay for the WT-B5 peptide, precautions were taken to ensure that similar experimental conditions (with respect to the number, average diameter, and curvature of liposomes in the field of view) were used (see Supplementary Material, Fig. S4). In each experiment, we chose regions of initially spherical liposomes (consisting of 100–120 closely packed liposomes). We acquired movies of each peptide solution that was introduced to the liposomes. For analyses, we visually counted the number of fusion events (a fusion event was defined as two liposomes merging into a new liposome with a larger diameter than each of the initial two liposomes), as well as the time of the event and the diameter of liposomes that fused. We defined the metric ''probability of fusion'' as the number of liposomes that fused divided by the total number of liposomes in the field of view; we used this value to compare results between fusion experiments.

To quantify two-dimensional aggregation of giant liposomes (e.g., in the case of Ca^{2+}-induced aggregation), we developed an image-processing algorithm using the PERL language (see Supplementary Material for detailed discussion of algorithm). This image-processing program analyzed phase-contrast micrographs of surface-attached giant liposomes and returned the value of ''percentage of shared membrane'' for the image. This metric was defined as the average percentage of each liposome that was directly in contact with adjacent liposomes.

RESULTS AND DISCUSSION

Formation of networks of surface-attached giant liposomes in microfluidic chambers

We formed cell-sized giant liposomes in transparent flow chambers by electroformation from spin-coated films of lipids on ITO electrodes (46). By growing liposomes from uniform films of lipids with optimal thickness, we obtained densely packed networks of giant liposomes (in which most liposomes were in close contact with several neighbors) across the entire surfaces of formation (Fig. 2 *A*) (45). We did not detach the liposomes; detachment is typically performed by applying a low frequency AC electric field (53). Instead, the giant liposomes remained affixed to the film of lipids on the surface of ITO by lipid tethers (45) even when exposed to flow. This experimental approach made it possible to monitor, in parallel, many membrane-membrane contacts between giant liposomes using a phase-contrast microscope. Additionally, we were able to observe the same region of

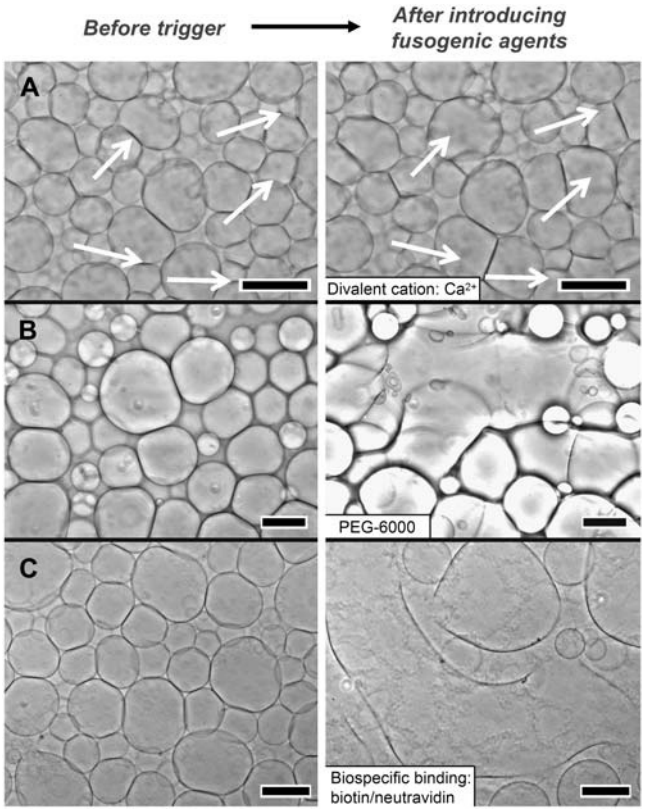

FIGURE 2 Triggering fusion by introducing fusogenic molecules to surface-attached giant liposomes. (*A*) Ca^{2+}-induced fusion: the introduction of 25 μM $CaCl_2$ promoted the fusion of 17% liposomes (composed of 90% POPC, 10% POPE) in the field of view. The arrows show the merging liposomes before introduction of Ca^{2+} (*left column*) and after 260 s of flow with a flow rate of 2.6 mL h^{-1} (*right column*). (*B*) Fusion triggered by a hydrophilic polymer: Flowing 10 mM PEG-6000 into the chamber induced the fusion of liposomes made of 90% POPC, 10% POPE. (*C*) Fusion triggered by biospecific interactions: Liposomes containing 95% POPC, 5% biotin-PE fused when 1.67 μM neutravidin was introduced to the chamber of liposomes. Initially spherical liposomes underwent several fusion events to form a single giant liposome (*right column* shows an intermediate stage in the fusion process). Scale bars = 50 μm. See Supplementary Material for complete movies of these processes.

liposomes upon introduction of new solutions to the flow chambers to follow directly the effect of the introduced molecules on membrane-membrane interactions and fusion. We used this setup in all subsequent fusion assays.

Ca^{2+}-induced fusion of giant liposomes

The fluidic setup presented here made it possible to rapidly investigate several fusogenic agents by simply flowing in solutions of the molecules and analyzing the resulting shape changes of the liposomes. To test the microfluidic fusion assay on a well-known process, we introduced Ca^{2+} ions to giant liposomes in the flow chamber. Calcium ions bind to the phosphate group of phospholipids, thus reducing charges at the surface of liposomes and promoting aggregations (54–56). In addition, Ca^{2+} can bridge the headgroups of adjacent vesicles and promote fusion through the creation of ''defects'' in neighboring bilayers (57). The formation of these defects, and hence fusion, is stochastic (57,58). When we introduced 25 μM $CaCl_2$ to giant liposomes, 17% of all liposomes in the field of view (total 164 with an average diameter of 30.6 $\pm$ 11.5 μm) fused within 1 h (see Supplementary Movie S1 for this Ca^{2+}-induced fusion). Most fusion events (85%) occurred in the first 8 min of flow (Fig. 2). In comparison, introducing 5 μM $CaCl_2$ triggered fusion of only 1.6% of liposomes (observing 128 liposomes with an average diameter of 33.4 $\pm$ 10.0 μm). These low probabilities of fusion highlight an advantage of directly examining many membrane-membrane interactions in parallel (59,60).

Two-dimensional aggregation of giant liposomes

Membrane fusion is preceded by close contact between adjacent membranes. Therefore, the tendency of membranes to aggregate in the absence or presence of ''membrane-active'' molecules is important to evaluate membrane-membrane interactions and fusion. We found that after introducing 25 μM $CaCl_2$ to giant liposomes and after the concomitant fusion of 17% of the liposomes, ~15% of liposomes underwent ''two-dimensional aggregation'' (Fig. 2 *A*, *right hand side*). In the context of this work, we defined two-dimensional aggregation as the changes in shape of surface-attached giant liposomes to increase contacts with neighboring liposomes (with all the liposomes imaged in the same two-dimensional plane, Fig. 2). These increased interactions had three characteristics: 1), the number of vesicle-vesicle contacts between liposomes that were initially not in contact increased (Supplementary Material, Fig. S1B); 2), vesicles adhered to one another (Supplementary Material, Fig. S1B); and 3), contact points between liposomes extended into defined lines (Fig. 3, *C* and *E*).

To examine this two-dimensional aggregation, we quantified the interactions between surface-attached giant liposomes in solutions of 0–200 mM $CaCl_2$ (Fig. 3). We developed an image processing algorithm to compute ''percentage of shared membrane'', which represents the average percentage of each visible liposome membrane in contact with adjacent liposome membranes (see Supplementary Material for a full discussion of image processing techniques). This quantification showed that giant liposomes exhibited significant two-dimensional aggregation between 100 μM and 1 mM $CaCl_2$ and also at $CaCl_2$ concentrations higher than 200 mM (Fig. 3 *A*). Interestingly, liposomes did not aggregate at an intermediate concentration of 10 mM $CaCl_2$ (Fig. 3 *D*), presumably due to binding of sufficient Ca^{2+} to the headgroups of lipids to induce positive-charge repulsion between bilayers (61).

By quantifying interactions between giant liposomes, we were able to compare this two-dimensional assay to other three-dimensional techniques. Previously, Akashi et al. monitored the adhesion of pairs of giant liposomes composed of

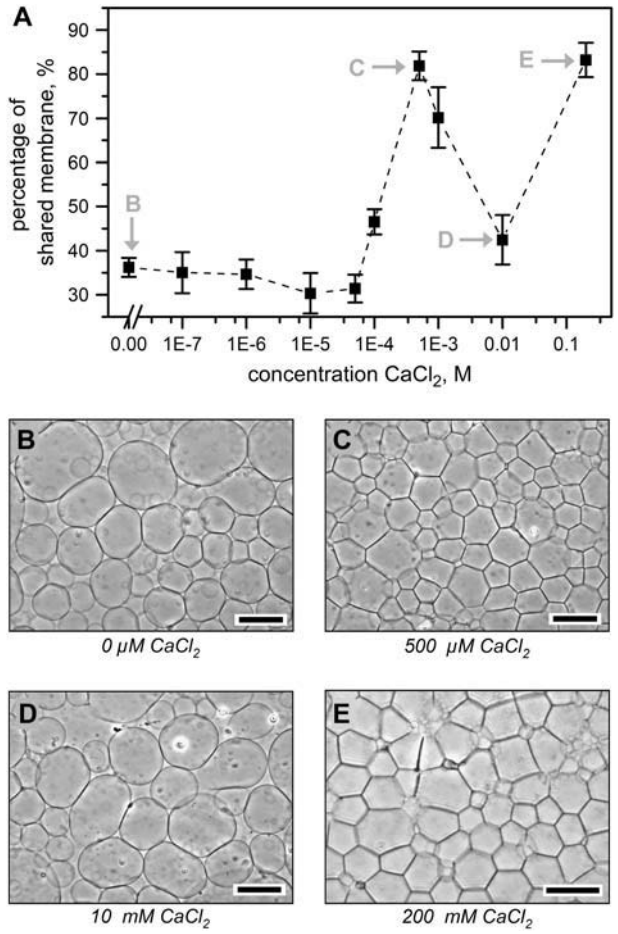

FIGURE 3 Quantification of Ca^{2+}-induced two-dimensional aggregation of surface-attached giant liposomes composed of 100% eggPC. (*A*) An image processing algorithm processed the micrographs of giant liposomes after 1 h of flow of $CaCl_2$ to determine the ''percentage of shared membrane'', which represents the average percentage of each liposome that is in contact with the visible membrane of adjacent liposomes ($N = 3$ for all points; error bars represent standard deviations). Images (*B–E*) show representative phase-contrast micrographs of two-dimensional aggregation after introducing solutions of (*B*) H_2O, (*C*) 500 μM $CaCl_2$, (*D*) 10 mM $CaCl_2$, and (*E*) 200 mM $CaCl_2$ to the liposomes. Note that the liposomes did not exhibit two-dimensional aggregation after introducing an intermediate concentration of 10 mM $CaCl_2$. Scale bars = 75 μm.

zwitterionic lipids in solutions of $CaCl_2$ (61). Liposomes adhered at concentrations of $CaCl_2$ between 50 μM to 1 mM and also at concentrations above 30 mM. Liposomes did not adhere at concentrations below 10 μM, and they also did not adhere at concentrations between 1 and 30 mM (61). Marra and Israelachvili obtained similar results using a direct force measuring apparatus on adsorbed planar lipid bilayers (62). Therefore, the results presented here for two-dimensional aggregation are in agreement with previous measurements of adhesion energies from Akashi et al. and from Marra and Israelachvili. With respect to comparing fusion in the two-dimensional case versus three-dimensional spectroscopic techniques, however, it is difficult to compare different fusion assays because several parameters (e.g., sizes of liposomes, composition of lipids) can drastically affect fusion (23,25). Most spectroscopic assays employ small and large unilamellar vesicles (SUVs and LUVs, respectively), which have significantly smaller sizes and higher curvature than the giant liposomes used here. Wilschut et al. suggested, however, that the tendency of vesicles to fuse after aggregation induced by Ca^{2+} is related to the tendency of vesicles to aggregate (63). Since aggregation was comparable between the assay presented here and previously reported three-dimensional techniques and since the presented assay shows that increasing the concentration of fusogenic agents such as Ca^{2+} increased the fusion probability, we suggest that the microfluidic two-dimensional fusion assay can deliver results that are at least qualitatively comparable to established fusion assays.

PEG-induced fusion: effects of osmotic mismatches

In addition to Ca^{2+}-induced fusion, we tested the assay with PEG. PEG is a hydrophilic polymer that has been employed to induce fusion of both cells and artificial vesicles (64). The well-known mechanism for PEG-triggered fusion derives from two effects: i), mechanical stress induced by the differences in osmolarity across the membranes of liposomes (65); and ii), dehydration of bilayers by PEG (66). In previous spectroscopic assays studying PEG-induced fusion, osmotic mismatches have been used to enhance fusion, as negative osmotic pressure (when the solution inside liposomes is hypotonic compared to the solution around liposomes, normally associated with shrinkage of liposomes) promoted fusion of LUVs in the presence of PEG (65).

Using the assay presented here, we first examined fusion of surface-attached giant liposomes after introducing osmotically unmatched solutions of PEG-6000 (at concentrations of 25 μM, 1 mM, 5 mM, 10 mM PEG-6000). Both 5 mM and 10 mM PEG induced massive fusion of giant liposomes (Fig. 2 *B*). In the case of 10 mM PEG, the liposomes appeared brighter than the surrounding PEG solution within 20 s after introducing 10 mM PEG to surface-attached liposomes; this difference was a result of mismatches in index of refraction of the PEG solution surrounding liposomes and the hypotonic solution inside the liposomes (Fig. 2 *B*, *left-hand side*) (45). Immediately after this gray-scale shift, liposomes fused massively with adjacent vesicles (Fig. 2 *B*, *right-hand side*). Concomitantly, the interactions between membranes increased strongly, and after 75 s, the majority (>75%) of the liposomes in the field of view had fused (some of these liposomes subsequently ruptured; see Supplementary Movie S2 for the full video of fusion). In contrast to the massive fusion triggered by 5 mM and 10 mM PEG, 25 μM PEG (a concentration that typically is far too low to trigger PEG-induced fusion) did not result in fusion or aggregation of giant liposomes (65).

In the case of 1 mM PEG-6000, however, giant liposomes shrank upon introduction of PEG. This shrinkage occurred on a timescale of minutes, and it was complete after ~20 min. Liposomes did not fuse, and we did not observe increased contacts between giant liposomes. Instead, the giant liposomes decreased their size such that only a few of them retained points of contact with neighboring giant liposomes. We attribute the absence of noticeable shrinkage of liposomes after introducing 5 and 10 mM PEG to the rapid fusion at these elevated concentrations. Presumably, in these cases, fusion occurred before significant shrinkage (due to osmotic mismatches) could occur.

We also examined PEG-induced fusion of giant liposomes using osmotically matched solutions of 1 mM, 5 mM, and 10 mM PEG-6000 (by forming liposomes in solutions of sucrose isoosmolal to the PEG solution to be introduced, see Supplementary Material, Fig. S3). With osmotically matched solutions, we observed that 5 mM and 10 mM PEG induced rapid fusion of giant liposomes. As expected, with osmotically matched 1 mM PEG, liposomes did not shrink. Instead, the liposomes experienced two-dimensional aggregation; we did not observe any fusion events within the field of view with 1 mM PEG.

Osmotic mismatches, therefore, can affect the results from the fusion assay presented here. To explore further the effects of osmotic mismatches by themselves, we created osmotic gradients (up to 5 mOsm/kg) with sucrose, a small nonfusogenic molecule. After introducing 5 mM sucrose to giant liposomes formed in 0.1 mM Tris, we did not observe any fusion events or aggregation. Most importantly, surface-attached giant liposomes did not shrink. Similarly, after reintroduction of 0.1 mM Tris to the chamber, the liposomes did not fuse or aggregate.

We attribute the absence of shrinkage or fusion of liposomes in the case of 5 mM sucrose to the presence of tubular openings that connect surface-attached giant liposomes to the film of lipids on the surface of the ITO electrode (45,53). Previously we showed that small solutes (including ions, sucrose, and water) exchanged rapidly through these tubules into (and out of) surface-attached liposomes; larger molecules (>3 kDa) did not exchange readily through these tubules (45). Therefore, as long as we were exchanging low molecular weight molecules (e.g., Ca^{2+} or sucrose) we observed only small, transient osmotic mismatches, as the tubular opening of the liposomes both allowed small molecules to enter liposomes and possibly also relieved osmotic pressure, thereby minimizing osmotic mismatches. Introducing 1 mM PEG-6000, however, did generate mismatches that were significant enough to shrink giant liposomes because the PEG did not exchange rapidly through the lipid tubules.

This example with PEG-6000 highlights several important aspects of the fusion assay presented here. First, when introducing macromolecules (>3 kDa), it is important to match osmolarities (unless the effects of osmotic mismatches are intended). For small molecular weight compounds (e.g., ions and sucrose) small mismatches in osmolarities do not cause shrinkage or swelling of vesicles because of lipid tubules that allow rapid diffusion into surface-attached liposomes. Second, to analyze aggregation and fusion, it is critically important to establish and maintain sufficient contacts between liposomes while introducing solutions to the flow chambers. Since the giant liposomes are surface attached in a two-dimensional matrix, they have limited lateral mobility to establish contacts with neighboring liposomes. Liposomes can either remain as they are, change their shape (e.g., by two-dimensional aggregation with neighbors), fuse, or shrink. Therefore, shrinkage of liposomes or examining fields of view with sparsely populated liposomes might generate nonrepresentative results since aggregation and fusion cannot occur if liposomes are spaced too far apart. For the fusion assays presented here, we always observed densely packed regions of giant liposomes (Fig. S4), and we only observed shrinkage of liposomes in the one case of introducing an unmatched solution of 1 mM PEG-6000. Despite these considerations, the presented aggregation and fusion assays are typically straightforward to perform since electroformation of giant liposomes from spin-coated films of lipids typically results in a dense two-dimensional network of surface-attached liposomes (45,46) and since matching osmolarities circumvents the problem of liposome shrinkage.

Fusion triggered by biospecific interactions

We utilized the strong binding interactions between biotin and neutravidin for triggering fusion and thus tested the microfluidic fusion assay on a reconstituted, minimal model of protein-mediated fusion. We formed surface-attached liposomes containing a biotinylated lipid and flowed a solution of 1.67 μM neutravidin in deionized water into the chamber (Fig. 2 *C*). Liposomes started to fuse immediately with their neighbors. This lateral fusion proceeded over 25 min until most liposomes (~80%) in the field of view had merged into one, large liposome with a diameter >600 μm (see Supplementary Movie S3 for a full movie of this fusion process). No lateral fusion of membranes occurred in a control experiment in which neutravidin was introduced to liposomes that did not contain biotin-PE.

The mechanism for this fusion process stems from biospecific interactions between adjacent membranes. Neutravidin has four binding sites with high affinity for biotin (67–69). When introduced to liposomes containing biotin-PE lipids, neutravidin presumably bound between adjacent liposomes, thus bringing the membranes into close contact. Once in contact, the membranes fused possibly due to the dehydration of membranes or from formation of defects by a large number of bridging molecules; several research groups showed previously that such defects can promote fusion (70–73). This neutravidin-driven mechanism may be considered as a minimal model of protein-mediated fusion in cells, such as fusion mechanisms based on SNARE complexes

(13,59,60). Liposome fusion by biotin-neutravidin interactions also complements studies of fusion of liposomes with complementary DNA on the headgroups of their lipids (39). The microfluidic fusion assay presented here makes it straightforward to investigate such minimalist models of biological fusion events, while providing the opportunity to increase the complexity of the model by introducing additional molecules.

Fusion assay for the WT-B5 peptide, which is involved in viral entry of herpes simplex virus

To demonstrate the usefulness of the presented microfluidic setup for characterizing novel, biologically relevant fusion processes, we performed a fusion assay with a 30-amino acid peptide (WT-B5 peptide) from the C-terminus of B5, a cell-surface membrane receptor protein that enables viral entry of HSV into host cells (52,74). The presence of synthetic WT-B5 peptide blocks HSV infection in human and other B5-expressing cells by competitive inhibition (52). Moreover, Perez et al. showed that high concentrations (~42 mM) of WT-B5 peptide was capable of fusing adjacent cells even in the absence of proteins from HSV (52). Here, we investigated the fusogenic activity of WT-B5 peptide on adjacent giant liposomes. This assay had the benefit that it proceeded under well-defined conditions of, e.g., membrane composition, buffer composition, and peptide concentration; we hypothesized, therefore, that it may make it possible to elucidate the contributions of individual molecules to the overall fusion event during viral entry of HSV.

We introduced WT-B5 peptide at concentrations between 0.5 and 25.0 μM to surface-attached giant liposomes. WT-B5 peptide induced fusion of giant liposomes, with a probability of fusion that was concentration dependent (Fig. 4 *A* and Supporting Movie S4). Maximal fusion occurred at 10 μM WT-B5 peptide, where the probability of fusion was 9.7%. Although a fusion probability below 10% was moderate, two-dimensional aggregation of membranes in the presence of the peptide occurred for all liposomes (Fig. 4 *B*). Even at 0.5 μM WT-B5 peptide, a concentration at which fusion was very rare, we observed significantly increased membrane-membrane interactions.

The rate of this two-dimensional liposome aggregation depended on the concentration of WT-B5 peptide. At 25 μM WT-B5 peptide, most (75%) of membranes deformed within 200 s across the entire field of view; at 0.5 μM, liposomes interacted gradually over the course of 1 h (flow rate for all concentrations: 2.6 mL h^{-1}). Interestingly, this aggregation was not reversible by flowing isoosmolar solutions of PBS through the chamber over the course of 2 h. This result indicated that a strong interaction occurs between WT-B5 peptide and adjacent liposome membranes composed of 90% POPC and 10% POPE.

We compared these results with fusion induced by two other short peptides with lengths and physicochemical properties similar to WT-B5 peptide (Table 1): ACTH (1–24); and the oxidized chain B of insulin (30 amino acids). The two control peptides each contained predicted regions of helix formation (similar to WT-B5 peptide, Table 1) (74–76). Utilizing the same experimental conditions as in studies of WT-B5 peptide, we found that these two peptides rarely triggered fusion of membranes (Fig. 4). We did, however, observe increased interactions between giant liposomes after introducing 5 μM concentrations of both the oxidized chain B of insulin and ACTH (1–24). ACTH (1–24) caused rapid deformation of membranes, and insulin chain B produced a more gradual interaction II than ACTH. Interestingly, this two-dimensional aggregation was reversible for both 5 μM ACTH (1–24) and 5 μM insulin chain B by flowing isoosmolar solutions of PBS through the chambers to flow out the peptide solutions. This result contrasts with irreversible membrane aggregation with 5 μM WT-B5 peptide under the same conditions, as mentioned above.

The results of this fusion assay for WT-B5 peptide suggest several characteristics about the interaction of this peptide with membranes. First, WT-B5 peptide interacts strongly with membranes of zwitterionic phospholipids such as PC and PE, possibly by partial insertion into these membranes. Second, membrane aggregation due to WT-B5 peptide was irreversible within 2 h, whereas this two-dimensional

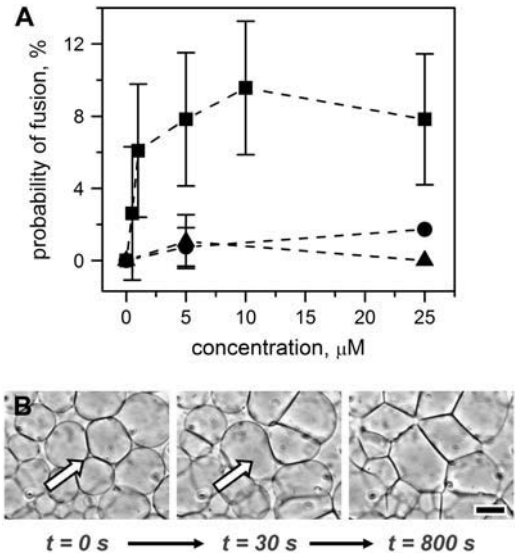

FIGURE 4 Fusion assay for WT-B5 peptide compared with control peptides using giant liposomes composed of 90% POPC, 10% POPE. (*A*) We measured the average probability of fusion (defined as the number of liposomes that fused divided by the total number of liposomes in the field of view) for different concentrations of (■) WT-B5 peptide, (●) ACTH (1–24), and (▲) the oxidized chain B of insulin. For WT-B5 peptide, the fusion probability was concentration dependent and enhanced compared to the control peptides. (*B*) The introduction of 5-μM WT-B5 peptide to initially spherical liposomes triggered the fusion of up to 10% of liposomes. The panels in *B* show a close-up of one of the fusion events at $t = 30$ s followed by increased interactions of membranes and two-dimensional aggregation over the course of the next 770 s. Scale bar = 40 μm.

TABLE 1 Sequence and structural properties of the peptides employed in fusion assay

Name of peptide	Sequence	Charge *	Average index of hydrophobicity *	Predicted structure in H_2O
WT-B5 peptide	KQQWQQLYDTLNAWKQN-LNKVKNSLLSLSD	+2	−2.7	Predicted α-helix and coiled-coil formation (52,74)
Oxidized chain B of insulin	FVNQHLC$_{ox}$GSHLVEALYL-VC$_{ox}$GERGF-FYTPKA	0	−0.8	Central α-helix (9–17) with well-defined β-turn (17–21) (76)
ACTH (1–24)	SYSMEHFRWGKPVGKKR-RPVKVYP	+6	−2.7	Hydrophobic regions (1–10) partition into POPC membrane (with potential helical structure), charged regions (11–24) associate with membrane surface (75)

*Charge and average index of hydrophobicity were computed using SAPS (statistical analysis of protein sequences) (82).

aggregation was reversible when induced by control peptides. Previous studies have indicated that other fusion peptides, such as HA, insert into bilayers and disrupt the packing of lipids (63,77). The observation that WT-B5 peptide induced fusion at a significantly higher probability than the control peptides supports the hypothesis that WT-B5 peptide inserts into membranes, whereas the control peptides appeared to associate peripherally or insert weakly into the membranes of liposomes (78–80).

A second implication of the results with WT-B5 peptide, which has been documented for other fusion peptides and molecules, is that aggregation of membranes induced by WT-B5 peptide is not sufficient to induce a high probability of fusion (81). Although almost all membranes aggregated at concentrations of WT-B5 peptide above 1 μM, the probabilities of fusion remained below 10%. Both control peptides also induced the two-dimensional aggregation of membranes but did not trigger fusion. Presumably, aggregation was due to dehydration of membranes combined with neutralization of surface charges on liposomes (from negatively charged impurities in PC lipids which are usually present) (55,63), and the formation of fusogenic defects was rare.

Finally, the results from this assay suggest that WT-B5 peptide by itself does not constitute the complete machinery necessary for effective viral fusion of HSV. Although WT-B5 peptide was successful in inducing some fusion of giant liposomes, these events were not as efficient as examples involving Ca^{2+} or biospecific tethering. Although the probabilities of fusion for 25 μM WT-B5 peptide were higher than for 25 μM PEG-6000, they were significantly lower than the probabilities for 25 μM Ca^{2+} or 1.67 μM neutravidin. It is likely that the addition of viral ligands or host cell proteins to the system would increase the probabilities of fusion. We believe that the fluidic assay presented here will be useful for the step-by-step reconstruction of parts of the fusion machinery of a range of fusion processes.

CONCLUSIONS

The capability to form closely packed giant liposomes that are attached to the surface of a flow chamber made it possible to develop a versatile and practical fusion assay. In this assay, possible fusogenic agents could be introduced into the chamber, and the fusogenic effects of these molecules could be observed on many membrane-membrane contacts in parallel. In addition, the microfluidic setup allowed exchanging solutions inside the chambers, leading to replacement of solutions both outside and inside surface-attached giant liposomes (45). This exchange of solutions allowed controlling the microenvironment around liposomes, making it possible to investigate membrane aggregation and fusion in a range of solutions with varying properties such as ionic strength (45), pH, or the presence of soluble molecules, peptides, proteins, etc.

Using this assay, we demonstrated that microfluidic assays of liposome fusion can reveal quantitative information on the probability of membrane fusion triggered by four different stimuli, including i), divalent cation-induced aggregation and destabilization of membranes; ii), dehydration of membranes by PEG; iii), receptor-mediated interactions between membranes; and iv), fusion promoted by a peptide involved in viral entry of HSV. Visualization of membrane fusion provided at least four advantages for studying membrane fusion. First, visualization was advantageous for studying the changes in shape of individual liposomes before fusion (e.g., two-dimensional aggregation, Fig. 3). Second, the fusion assay presented here provided information about the individual size of each liposome that fused, as well as the time after introduction of the fusogenic agent. Third, using surface-attached giant liposomes may allow monitoring changes in the shapes of liposomes during the fusion process. In a recent article, Lei and MacDonald used high-speed microfluorescence spectroscopy to study intermediate lipid-mixing structures in the fusion of giant liposomes (40). It is conceivable that high-speed phase-contrast microscopy techniques could reveal useful information about the changes in shape of giant liposomes in response to introduced fusogenic agents before and during fusion, using the assay presented here. And fourth, being able to observe the fusion process provided information about the mechanism of fusion events. In the case of the WT-B5 peptide, the concentration-dependent, irreversible two-dimensional aggregation of

membranes indicated that this peptide interacts strongly with and possibly partitions into bilayers. This interaction was sufficient to induce fusion of giant liposomes but not to the extent to conclude that WT-B5 peptide by itself is a highly efficient fusion peptide.

Despite these numerous advantages, several aspects of this assay could be further improved. The current methods that we used for quantifying fusion required detecting and measuring fusion events visually, and this analysis can be time consuming. We believe, however, that image processing algorithms can be developed (perhaps similar to the algorithms we present in the Supplementary Material to quantify two-dimensional aggregation) to detect fusion in an automated procedure to simplify and accelerate the analysis. Also, the assay in its present form does not reveal quantitative information on lipid and contents mixing, two parameters that can provide kinetic information in spectroscopic assays (27). Therefore, existing spectroscopic techniques may currently offer rapid means to quantify fusion, whereas the assay presented here enables direct visualization of fusion events or aggregation of cell-sized giant vesicles. We believe that triggering and observing membrane fusion in microfluidic chambers provides a broadly applicable and straightforward procedure for performing fusion assays on cell-sized liposomes under well-defined and variable conditions.

SUPPLEMENTARY MATERIAL

An online supplement to this article can be found by visiting BJ Online at http://www.biophysj.org.

We thank Amy P. Wong for her insightful suggestions, Shuichi Takayama for use of the spin-coater, and Jodi L. Liu for her careful measurements.

This work was supported by the National Science Foundation (02-111 CAREER Award, M.M.). D.J.E. acknowledges a National Institutes of Health Cellular Biotechnology Training Program (CBTP) fellowship and a Rackham Graduate Fellowship at the University of Michigan. S.R.L. acknowledges the Genetics Training Program and a Rackham graduate fellowship at the University of Michigan.

REFERENCES

1. Chen, E. H., and E. N. Olson. 2005. Unveiling the mechanisms of cell-cell fusion. *Science*. 308:369–373.
2. Fujii, G. 1999. To fuse or not to fuse: the effects of electrostatic interactions, hydrophobic forces, and structural amphiphilicity on protein-mediated membrane destabilization. *Adv. Drug Deliv. Rev.* 38:257–277.
3. Gennis, R. B. 1989. Biomembranes: molecular structure and function. C. R. Cantor, editor. Springer-Verlag, New York. 533.
4. Kemble, G. W., T. Danieli, and J. M. White. 1994. Lipid-anchored influenza hemagglutinin promotes hemifusion, not complete fusion. *Cell*. 76:383–391.
5. Cevc, G., and H. Richardsen. 1999. Lipid vesicles and membrane fusion. *Adv. Drug Deliv. Rev.* 38:207–232.
6. Jahn, R., T. Lang, and T. C. Sudhof. 2003. Membrane fusion. *Cell*. 112:519–533.
7. Tamm, L. K., J. Crane, and V. Kiessling. 2003. Membrane fusion: a structural perspective on the interplay of lipids and proteins. *Curr. Opin. Struct. Biol.* 13:453–466.
8. Bentz, J. 2000. Membrane fusion mediated by coiled coils: a hypothesis. *Biophys. J.* 78:886–900.
9. Smith, A. E., and A. Helenius. 2004. How viruses enter animal cells. *Science*. 304:237–242.
10. Lee, J., and B. R. Lentz. 1997. Evolution of lipidic structures during model membrane fusion and the relation of this process to cell membrane fusion. *Biochemistry*. 36:6251–6259.
11. Lentz, B. R., and J. K. Lee. 1999. Poly(ethylene glycol) (PEG)-mediated fusion between pure lipid bilayers: a mechanism in common with viral fusion and secretory vesicle release? (Review). *Mol. Membr. Biol.* 16:279–296.
12. Chernomordik, L. V., G. B. Melikyan, and Y. A. Chizmadzhev. 1987. Biomembrane fusion: a new concept derived from model studies using two interacting planar lipid bilayers. *Biochim. Biophys. Acta*. 906:309–352.
13. Weber, T., B. V. Zemelman, J. A. McNew, B. Westermann, M. Gmachl, F. Parlati, T. H. Sollner, and J. E. Rothman. 1998. SNAREpins: minimal machinery for membrane fusion. *Cell*. 92:759–772.
14. Cohen, F. S., M. H. Akabas, and A. Finkelstein. 1982. Osmotic swelling of phospholipid-vesicles causes them to fuse with a planar phospholipid-bilayer membrane. *Science*. 217:458–460.
15. Cohen, F. S., J. Zimmerberg, and A. Finkelstein. 1980. Fusion of phospholipid-vesicles with planar phospholipid-bilayer membranes. 2. Incorporation of a vesicular membrane marker into the planar membrane. *J. Gen. Physiol.* 75:251–270.
16. Helm, C. A., J. N. Israelachvili, and P. M. McGuiggan. 1992. Role of hydrophobic forces in bilayer adhesion and fusion. *Biochemistry*. 31: 1794–1805.
17. Tanaka, T., and M. Yamazaki. 2004. Membrane fusion of giant unilamellar vesicles of neutral phospholipid membranes induced by La3+. *Langmuir*. 20:5160–5164.
18. Nir, S., J. Bentz, J. Wilschut, and N. Duzgunes. 1983. Aggregation and fusion of phospholipid-vesicles. *Prog. Surf. Sci.* 13:1–124.
19. Bentz, J., D. Alford, J. Cohen, and N. Duzgunes. 1988. La-3+-induced fusion of phosphatidylserine liposomes—close approach, intermembrane intermediates, and the electrostatic surface-potential. *Biophys. J.* 53:593–607.
20. Lee, J., and B. R. Lentz. 1998. Secretory and viral fusion may share mechanistic events with fusion between curved lipid bilayers. *Proc. Natl. Acad. Sci. USA*. 95:9274–9279.
21. Munro, J. C., and C. W. Frank. 2004. In situ formation and characterization of poly(ethylene glycol)-supported lipid bilayers on gold surfaces. *Langmuir*. 20:10567–10575.
22. Zimmermann, U. 1982. Electric field-mediated fusion and related electrical phenomena. *Biochim. Biophys. Acta*. 694:227–277.
23. Bentz, J., and N. Duzgunes. 1985. Fusogenic capacities of divalent-cations and effect of liposome size. *Biochemistry*. 24:5436–5443.
24. Wilschut, J., N. Duzgunes, and D. Papahadjopoulos. 1981. Calcium-magnesium specificity in membrane-fusion—kinetics of aggregation and fusion of phosphatidylserine vesicles and the role of bilayer curvature. *Biochemistry*. 20:3126–3133.
25. Ohki, S. 1984. Effects of divalent-cations, temperature, osmotic-pressure gradient, and vesicle curvature on phosphatidylserine vesicle fusion. *J. Membr. Biol.* 77:265–275.
26. Lentz, B. R., G. F. McIntyre, D. J. Parks, J. C. Yates, and D. Massenburg. 1992. Bilayer Curvature and Certain Amphipaths promote poly(ethylene glycol)-induced fusion of dipalmitoylphosphatidylcholine unilamellar vesicles. *Biochemistry*. 31:2643–2653.
27. Evans, K. O., and B. R. Lentz. 2002. Kinetics of lipid rearrangements during poly(ethylene glycol)-mediated fusion of highly curved unilamellar vesicles. *Biochemistry*. 41:1241–1249.
28. Duzgunes, N., T. M. Allen, J. Fedor, and D. Papahadjopoulos. 1987. Lipid mixing during membrane aggregation and fusion—why fusion assays disagree. *Biochemistry*. 26:8435–8442.

29. Ellens, H., J. Bentz, and F. C. Szoka. 1985. H+-Induced and Ca-2+-induced fusion and destabilization of liposomes. *Biochemistry.* 24:3099–3106.

30. Wilschut, J., and D. Papahadjopoulos. 1979. Ca2+-induced fusion of phospholipid-vesicles monitored by mixing of aqueous contents. *Nature.* 281:690–692.

31. Trivedi, V. D., C. Yu, B. Veeramuthu, S. Francis, and D. K. Chang. 2000. Fusion induced aggregation of model vesicles studied by dynamic and static light scattering. *Chem. Phys. Lipids.* 107:99–106.

32. Murata, M., S. Takahashi, S. Kagiwada, A. Suzuki, and S. Ohnishi. 1992. Ph-dependent membrane-fusion and vesiculation of phospholipid large unilamellar vesicles induced by amphiphilic anionic and cationic peptides. *Biochemistry.* 31:1986–1992.

33. Siegel, D. P., J. L. Burns, M. H. Chestnut, and Y. Talmon. 1989. Intermediates in membrane-fusion and bilayer nonbilayer phase-transitions imaged by time-resolved cryo-transmission electron-microscopy. *Biophys. J.* 56:161–169.

34. Nomura, F., T. Inaba, S. Ishikawa, M. Nagata, S. Takahashi, H. Hotani, and K. Takiguchi. 2004. Microscopic observations reveal that fusogenic peptides induce liposome shrinkage prior to membrane fusion. *Proc. Natl. Acad. Sci. USA.* 101:3420–3425.

35. Soltesz, S. A., and D. A. Hammer. 1997. Lysis of large unilamellar vesicles induced by analogs of the fusion peptide of influenza virus hemagglutinin. *J. Colloid Interface Sci.* 186:399–409.

36. Soltesz, S. A., and D. A. Hammer. 1995. Micropipette manipulation technique for the monitoring of pH-dependent membrane lysis as induced by the fusion peptide of influenza-virus. *Biophys. J.* 68: 315–325.

37. Akashi, K., H. Miyata, H. Itoh, and K. Kinosita. 1996. Preparation of giant liposomes in physiological conditions and their characterization under an optical microscope. *Biophys. J.* 71:3242–3250.

38. Shoemaker, S. D., and T. K. Vanderlick. 2002. Intramembrane electrostatic interactions destabilize lipid vesicles. *Biophys. J.* 83:2007–2014.

39. Heuvingh, J., F. Pincet, and S. Cribier. 2004. Hemifusion and fusion of giant vesicles induced by reduction of inter-membrane distance. *Eur. Phys. J. E. Soft Matter.* 14:269–276.

40. Lei, G. H., and R. C. MacDonald. 2003. Lipid bilayer vesicle fusion: intermediates captured by high-speed microfluorescence spectroscopy. *Biophys. J.* 85:1585–1599.

41. Chiu, D. T. 2001. A microfluidics platform for cell fusion—commentary. *Curr. Opin. Chem. Biol.* 5:609–612.

42. Chiu, D. T., C. F. Wilson, F. Ryttsen, A. Stromberg, C. Farre, A. Karlsson, S. Nordholm, A. Gaggar, B. P. Modi, A. Moscho, R. A. Garza-Lopez, O. Orwar, and R. N. Zare. 1999. Chemical transformations in individual ultrasmall biomimetic containers. *Science.* 283:1892–1895.

43. Stromberg, A., A. Karlsson, F. Ryttsen, M. Davidson, D. T. Chiu, and O. Orwar. 2001. Microfluidic device for combinatorial fusion of liposomes and cells. *Anal. Chem.* 73:126–130.

44. Stromberg, A., F. Ryttsen, D. T. Chiu, M. Davidson, P. S. Eriksson, C. F. Wilson, O. Orwar, and R. N. Zare. 2000. Manipulating the genetic identity and biochemical surface properties of individual cells with electric-field-induced fusion. *Proc. Natl. Acad. Sci. USA.* 97: 7–11.

45. Estes, D. J., and M. Mayer. 2005. Giant liposomes in physiological buffer using electroformation in a flow chamber. *Biochim. Biophys. Acta.* 1712:152–160.

46. Estes, D. J., and M. Mayer. 2005. Electroformation of giant liposomes from spin-coated films of lipids. *Colloids Surf. B Biointerfaces.* 42:115–123.

47. Lee, J. N., C. Park, and G. M. Whitesides. 2003. Solvent compatibility of poly(dimethylsiloxane)-based microfluidic devices. *Anal. Chem.* 75:6544–6554.

48. Angelova, M. I., and D. S. Dimitrov. 1986. Liposome electroformation. *Faraday Discuss. Chem. Soc.* 81:303–311.

49. Angelova, M., S. Soleau, P. Meleard, J. F. Faucon, and P. Bothorel. 1992. Preparation of giant vesicles by external AC electric fields. Kinetics and applications. *Prog. Colloid Polym. Sci.* 89:127–131.

50. Menger, F. M., and M. I. Angelova. 1998. Giant vesicles: imitating the cytological processes of cell membranes. *Acc. Chem. Res.* 31:789–797.

51. Bagatolli, L. A., T. Parasassi, and E. Gratton. 2000. Giant phospholipid vesicles: comparison among the whole lipid sample characteristics using different preparation methods—a two photon fluorescence microscopy study. *Chem. Phys. Lipids.* 105:135–147.

52. Perez, A., Q. X. Li, P. Perez-Romero, G. DeLassus, S. R. Lopez, S. Sutter, N. McLaren, and A. O. Fuller. 2005. A new class of receptor for herpes simplex virus has heptad repeat motifs that are common to membrane fusion proteins. *J. Virol.* 79:7419–7430.

53. Angelova, M. I. 2000. Liposome electroformation. *In* Giant Vesicles. P. L. Luisi, and P. Walde, editors. John Wiley & Sons, New York. 27–36.

54. Ohki, S., and N. Duzgunes. 1979. Divalent cation-induced interaction of phospholipid vesicle and monolayer membranes. *Biochim. Biophys. Acta.* 552:438–449.

55. Pincet, F., S. Cribier, and E. Perez. 1999. Bilayers of neutral lipids bear a small but significant charge. *Eur. Phys. J. B.* 11:127–130.

56. McLaughlin, A., C. Grathwohl, and S. McLaughlin. 1978. Adsorption of divalent-cations to phosphatidylcholine bilayer membranes. *Biochim. Biophys. Acta.* 513:338–357.

57. Papahadjopoulos, D., S. Nir, and N. Duzgunes. 1990. Molecular mechanisms of calcium-induced membrane-fusion. *J. Bioenerg. Biomembr.* 22:157–179.

58. Rand, R. P., B. Kachar, and T. S. Reese. 1985. Dynamic morphology of calcium-induced interactions between phosphatidylserine vesicles. *Biophys. J.* 47:483–489.

59. Fix, M., T. J. Melia, J. K. Jaiswal, J. Z. Rappoport, D. Q. You, T. H. Sollner, J. E. Rothman, and S. M. Simon. 2004. Imaging single membrane fusion events mediated by SNARE proteins. *Proc. Natl. Acad. Sci. USA.* 101:7311–7316.

60. Liu, T., W. C. Tucker, A. Bhalla, E. R. Chapman, and J. C. Weisshaar. 2005. SNARE-driven, 25-millisecond vesicle fusion in vitro. *Biophys. J.* biophysj.105.062539.

61. Akashi, K., H. Miyata, H. Itoh, and K. Kinosita. 1998. Formation of giant liposomes promoted by divalent cations: critical role of electrostatic repulsion. *Biophys. J.* 74:2973–2982.

62. Marra, J., and J. Israelachvili. 1985. Direct measurements of forces between phosphatidylcholine and phosphatidylethanolamine bilayers in aqueous-electrolyte solutions. *Biochemistry.* 24:4608–4618.

63. Wilschut, J., and D. Hoekstra. 1986. Membrane-fusion—lipid vesicles as a model system. *Chem. Phys. Lipids.* 40:145–166.

64. Lentz, B. R. 1994. Polymer-induced membrane-fusion—potential mechanism and relation to cell-fusion events. *Chem. Phys. Lipids.* 73: 91–106.

65. Malinin, V. S., P. Frederik, and B. R. Lentz. 2002. Osmotic and curvature stress affect PEG-induced fusion of lipid vesicles but not mixing of their lipids. *Biophys. J.* 82:2090–2100.

66. Boni, L. T., T. P. Stewart, J. L. Alderfer, and S. W. Hui. 1981. Lipid-polyethylene glycol interactions.1. Induction of fusion between liposomes. *J. Membr. Biol.* 62:65–70.

67. Livnah, O., E. A. Bayer, M. Wilchek, and J. L. Sussman. 1993. Three-dimensional structures of avidin and the avidin-biotin complex. *Proc. Natl. Acad. Sci. USA.* 90:5076–5080.

68. Weber, P. C., D. H. Ohlendorf, J. J. Wendoloski, and F. R. Salemme. 1989. Structural origins of high-affinity biotin binding to streptavidin. *Science.* 243:85–88.

69. Vanroy, N., K. Mangelschots, and F. Speleman. 1993. Improved immunocytochemical detection of biotinylated probes with neutralite avidin. *Trends Genet.* 9:71–72.

70. Safran, S. A., T. L. Kuhl, and J. N. Israelachvili. 2001. Polymer-induced membrane contraction, phase separation, and fusion via Marangoni flow. *Biophys. J.* 81:659–666.

71. Helm, C. A., J. N. Israelachvili, and P. M. McGuiggan. 1989. Molecular mechanisms and forces involved in the adhesion and fusion of amphiphilic bilayers. *Science*. 246:919–922.

72. Tieleman, D. P., and J. Bentz. 2002. Molecular dynamics simulation of the evolution of hydrophobic defects in one monolayer of a phosphatidylcholine bilayer: relevance for membrane fusion mechanisms. *Biophys. J*. 83:1501–1510.

73. Stevens, M. J., J. H. Hoh, and T. B. Woolf. 2003. Insights into the molecular mechanism of membrane fusion from simulation: evidence for the association of splayed tails. *Phys. Rev. Lett.* 91:188102

74. Perez-Romero, P., and A. O. Fuller. 2005. The C terminus of the B5 receptor for herpes simplex virus contains a functional region important for infection. *J. Virol.* 79:7431–7437.

75. Gao, X. F., and T. C. Wong. 1998. Studies of the binding and structure of adrenocorticotropin peptides in membrane mimics by NMR spectroscopy and pulsed-field gradient diffusion. *Biophys. J*. 74:1871–1888.

76. Hawkins, B., K. Cross, and D. Craik. 1995. Solution structure of the B-chain of insulin as determined by 1H NMR spectroscopy. Comparison with the crystal structure of the insulin hexamer and with the solution structure of the insulin monomer. *Int. J. Pept. Protein Res*. 46:424–433.

77. Longo, M. L., A. J. Waring, and D. A. Hammer. 1997. Interaction of the influenza hemagglutinin fusion peptide with lipid bilayers: area expansion and permeation. *Biophys. J*. 73:1430–1439.

78. Bechinger, B. 1999. The structure, dynamics and orientation of antimicrobial peptides in membranes by multidimensional solid-state NMR spectroscopy. *Biochim. Biophys. Acta*. 1462:157–183.

79. Zuckermann, M. J., and T. Heimburg. 2001. Insertion and pore formation driven by adsorption of proteins onto lipid bilayer membrane-water interfaces. *Biophys. J*. 81:2458–2472.

80. Shai, Y. 1999. Mechanism of the binding, insertion and destabilization of phospholipid bilayer membranes by alpha-helical antimicrobial and cell non-selective membrane-lytic peptides. *Biochim. Biophys. Acta.* 1462:55–70.

81. Papahadjopoulos, D., W. J. Vail, C. Newton, S. Nir, K. Jacobson, G. Poste, and R. Lazo. 1977. Studies on membrane-fusion. 3. Role of calcium-induced phase-changes. *Biochim. Biophys. Acta*. 465:579–598.

82. Brendel, V., P. Bucher, I. R. Nourbakhsh, B. E. Blaisdell, and S. Karlin. 1992. Methods and algorithms for statistical-analysis of protein sequences. *Proc. Natl. Acad. Sci. USA*. 89:2002–2006.